

Soil moisture data as a constraint for groundwater recharge estimation

Simon A. Mathias^{a,*}, James P. R. Sorensen^b, Adrian P. Butler^c

^a*Department of Earth Sciences, Durham University, Durham, UK*

^b*British Geological Survey, Maclean Building, Wallingford, UK*

^c*Department of Civil and Environmental Engineering, Imperial College London, London, UK*

Abstract

Estimating groundwater recharge rates is important for water resource management studies. Modeling approaches to forecast groundwater recharge typically require observed historic data to assist calibration. It is generally not possible to observe groundwater recharge rates directly. Therefore, in the past, much effort has been invested to record soil moisture content (SMC) data, which can be used in a water balance calculation to estimate groundwater recharge. In this context, SMC data is measured at different depths and then typically integrated with respect to depth to obtain a single set of aggregated SMC values, which are used as an estimate of the total water stored within a given soil profile. This article seeks to investigate the value of such aggregated SMC data for conditioning groundwater recharge models in this respect. A simple modeling approach is adopted, which utilizes an emulation of Richards' equation in conjunction with a soil texture pedotransfer function. The only unknown parameters are soil texture. Monte Carlo simulation is performed for four different SMC monitoring sites. The model is used to estimate both aggregated SMC and groundwater recharge. The impact of conditioning the model to the aggregated SMC data is then explored in terms of its ability to reduce the uncertainty associated with recharge estimation. Whilst uncertainty in soil texture can lead to significant uncertainty in groundwater

23 recharge estimation, it is found that aggregated SMC is virtually insensitive to soil texture.
24 *Keywords:* Conditioning, Groundwater recharge, Soil moisture content, Soil texture, Vertical
25 percolation

26 **1. Introduction**

27 An essential aspect of water resource planning often involves the estimation of groundwater
28 recharge rates, here defined as the rate at which water arrives at the water table of an aquifer
29 following precipitation, interception, snow melt, evapotranspiration and percolation through the
30 unsaturated zone. In many cases, water loss during percolation through the unsaturated zone
31 below the reach of plant roots can be assumed negligible. Consequently, vertical percolation
32 beneath the reach of plant roots and groundwater recharge are often treated as being the same
33 (Quinn et al., 2012; Sorensen et al., 2014). Hereafter, vertical percolation is referred to as a proxy
34 for groundwater recharge. Vertical percolation rates (VPR) can be estimated using a multitude
35 of different models, all of which require historic data of some form to enable appropriate model
36 parameter calibration.

37 Ideally, such models should be calibrated to observed groundwater recharge rates. However,
38 groundwater recharge data is difficult to observe directly. Some studies have sought to derive
39 recharge data by separating out base flow from river discharge rate records (Rutledge, 2007). The
40 problem here is that base flow separation methods are, in themselves, *ad hoc* and unconstrained,
41 unless combined with some form of tracer based mass balance study (Lott and Stewart, 2016).
42 Another method is to assume a specific yield for an unconfined aquifer and to infer recharge rates

*Corresponding author. Tel.: +44 (0)1913343491, Fax: +44 (0)1913342301, E-mail address: s.a.mathias@durham.ac.uk

43 from water table changes (Healy and Cook, 2002). The problem with this latter approach is that
44 there is often significant uncertainty about the time-varying characteristics of specific yield (Healy
45 and Cook, 2002; Mathias and Butler, 2006) and significant care is required to properly take into
46 account the effects of lateral groundwater flow rates (Healy and Cook, 2002; Cuthbert et al., 2016).

47 Arguably, the most direct method of observing recharge rates is to measure VPR from an in
48 situ lysimeter (von Freyberg et al., 2015). The issue here is that such facilities are very expensive
49 to manage and very few facilities exist around the world.

50 Another related approach is to continuously monitor moisture content within a soil profile over
51 a long period of time (Ireson et al., 2006). Providing that precipitation (net of interception) and
52 actual evapotranspiration (AE) are also monitored, soil moisture content (SMC) data can be used
53 to develop a VPR measurement by water balance. However, a problem is that AE is not often mea-
54 sured. Instead, an estimate of potential evapotranspiration (PE) is generally obtained using weather
55 station data (incoming radiation, temperature, humidity, wind speed etc.) in conjunction with an
56 appropriate physics model (e.g. Allen et al., 1998). Under such conditions, a direct estimate of
57 VPR is not possible by water balance, as the quantity of AE is unknown. Consequently, VPR must
58 instead be estimated by simulating soil-plant-water processes using an appropriate model, which
59 is conditioned to the observed SMC data.

60 Interestingly, previous modeling studies have focused on the ability of models to estimate SMC
61 data as opposed to the value of SMC data as a conditioner for estimating VPR (Ragab et al., 1997;
62 Sorensen et al., 2014). In a recent study, Sorensen et al. (2014) presented SMC content data from
63 four instrumented sites from southern England. They then compared estimated SMC data from
64 four different uncalibrated recharge estimation methods. The authors conclude that, whilst each of

65 four models provided a “generally good agreement” between simulated and observed SMC, there
66 were large discrepancies between the different VPR estimates, leading to concerns over the value
67 of SMC data for conditioning groundwater recharge modeling in the future.

68 In the current study, the four aforementioned instrumented sites presented by Sorensen et al.
69 (2014) are revisited to quantify the extent to which observed SMC data can be used to reduce
70 uncertainty associated with groundwater recharge in the context of a single model structure. In
71 particular, the model structure used includes a recently developed soil moisture accounting pro-
72 cedure (SMAP) designed by Mathias et al. (2015), which is described later on in this article.
73 Unknown input parameters associated with this SMAP only include information about the soil
74 texture of the site (i.e., % clay, % silt and % sand).

75 The outline of this article is as follows. An explanation is provided concerning the data, models
76 and conditioning strategies to be applied. The aforementioned SMAP is used to estimate VPR at
77 the four instrumented sites in southern England. Probability of non-exceedance (PNE) confidence
78 limits are acquired using four successive methodologies. For comparison, PNE confidence limits
79 are first acquired assuming any soil texture is equally likely to be applicable at each of the four
80 sites. PNE confidence limits are then refined by conditioning the SMAP to the observed SMC
81 data from each site. For further comparison, an additional set of PNE confidence limits is acquired
82 by restricting soil texture to be within a polygon on a soil texture ternary diagram associated with
83 the soil texture classification for that site as designated by the UK soil observatory (UKSO). The
84 results are compared and contrasted so as to draw wider conclusions with regards to the value of
85 observed SMC data when seeking to estimate VPR for groundwater recharge studies in the future.

86 **2. Data and methodology**

87 *2.1. Data*

88 The data used for this study include daily net rainfall (i.e., rainfall minus canopy interception
89 losses) and PE data in conjunction with observed SMC from the four instrumented sites previously
90 discussed by Sorensen et al. (2014). The four sites include Warren Farm, Highfield Farm, Beche
91 Park Wood and Grimsbury Wood, all of which are located in Berkshire, UK.

92 Daily net rainfall and AE data were obtained by Sorensen et al. (2014) using JULES (Best
93 et al., 2011) driven by nearby meteorological observations. A default JULES parameterisation
94 was used for grassland sites with woodland vegetation parameters defined using observations by
95 Herbst et al. (2008).

96 Routine SMC data were obtained at each site as follows (Sorensen et al., 2014). Point mea-
97 surements of SMC were obtained using neutron probes at 17 intervals at depths of 0.1, 0.2, 0.3,
98 0.4, 0.5, 0.6, 0.8, 1.0, 1.2, 1.4, 1.6, 1.8, 2.0, 2.3, 2.6, 2.9, 3.2 m, respectively. The results were then
99 aggregated together, by depth weighting, to obtain a depth of water contained within the top 3 m
100 of the soil profile.

101 Soil texture maps from the UK soil observatory (UKSO, 2016) were used to provide soil texture
102 data describing the surface cover of the four sites.

103 The UKSO map covers Great Britain and integrates geology and soil characteristics at a scale
104 of 1:50 000, with a 1 km resolution version available for regional overviews. The simplified soil
105 texture classifications are derived from measured soil textures (% clay, % silt and % sand) taken
106 from archive samples held by the British Geological Survey. The map uses terms that refer to:

107 sandy soils, silty soils, clayey soils and loamy soils with additional indicators for the presence of
108 chalk fragments (chalky) and peat (peaty). For reference, soil texture ternary diagrams illustrating
109 the various available UKSO soil texture classifications are presented in Fig. 1.

110 2.2. *Geology and soil cover of the field sites*

111 Location maps of the four field sites, Warren Farm, Highfield Farm, Beche Park Wood and
112 Grimsbury Wood, have previously been presented by Sorensen et al. (2014). The four locations
113 cover a range of different superficial geology, soil type and land use. Warren Farm and Highfield
114 Farm are grassland sites. Beche Park Wood and Grimsbury Wood are deciduous woodland sites.
115 All four sites are underlain by chalk geology, with water tables located at greater than 10 m depth.
116 The Chalk in this area is overlain by superficial clay-with-flints formation or Paleogene deposits
117 comprising of clays, interbedded sands and silty clays with the exception of Warren Farm which
118 is chalk outcrop (Sorensen et al., 2014).

119 Soil logs indicate the following (Sorensen et al., 2014): Warren Farm consists of a thin 0.2 m
120 soil, including flints, overlying weathered chalk which grades into consolidated chalk between 1
121 and 3 m depth. Highfield Farm consists of a very heterogeneous fine loam to around 0.4 to 0.5 m,
122 above clay with various degrees of interbedded gravel. Beche Park Wood consists of around 0.3 m
123 of gravely clay, over clay-with-flints containing occasional sand filled fissures. Grimsbury Wood
124 is predominantly silty clay overlain by 0.3 m of loam.

125 The soil texture for the four sites according to UKSO is as follows: Warren Farm is described
126 as a “chalky silty loam”. Highfield Farm is described as “loam to sand”. Beche Park Wood is
127 described as “clay to clayey loam”. Grimsbury Wood is described as “clay to silt”.

128 The UKSO map provides quite reasonable soil texture descriptions for Beche Park Wood and
129 Grimsbury Wood. However, the UKSO map soil texture descriptions do not compare well with
130 the field descriptions for Warren Farm and Highfield Farm, previously provided by Sorensen et
131 al. (2014). Indeed there are many problems associated with determining soil texture for soils
132 associated with chalk (Kerry et al., 2009). Nevertheless, the UKSO soil textures will be considered
133 further as an alternative conditioner for groundwater recharge estimation.

134 *2.3. Vertical percolation rate (VPR) modeling*

135 The soil moisture accounting procedure (SMAP) previously proposed by Mathias et al. (2015)
136 was used to simulate VPR at the four sites. The model requires daily net rainfall, PE data and soil
137 texture data to provide estimates of aggregated SMC and VPR.

138 The SMAP has been specifically designed to emulate Richards' equation in conjunction with
139 the plant roots stress function of Feddes et al. (1976) and the pedotransfer function stored within
140 the ROSETTA database (Schaap et al., 2001). The associated conceptual model comprises a 3
141 m thick homogenous soil column with an exponentially distributed vertical plant root density
142 distribution contained within the top 1 m of soil. The upper boundary condition comprises a flux
143 associated with the net rainfall rate. The lower boundary condition is represented as a gravity
144 drainage boundary.

145 An aspect not adequately discussed by Mathias et al. (2015) is the stability of the Euler explicit
146 time-stepping scheme used within the SMAP. Stability is ensured using a scheme very similar to
147 that presented in Appendices B and C of Mathias et al., (2016). Further details about how this is
148 achieved are provided in Appendix A of this article.

149 Each SMAP simulation was run for a warm-up period of at least 90 days before simulating the
150 period through which observed SMC data is available. An initial value of SMC used to start the
151 warm-up simulation was obtained as follows: First, the SMC that would be expected for a 3 m soil
152 column at hydrostatic conditions with a fictitious water table present at 2 m below the base of the
153 column was determined. The SMAP was then run, with this starting SMC value, using the first
154 three years of net-rainfall and PE data. The final SMC value from this latter simulation was then
155 used as the starting SMC value for the beginning of the 90 day warm-up period.

156 *2.4. Determination of VPR confidence limits*

157 Unconstrained probabilistic estimates of VPR are obtained by performing a Monte Carlo sim-
158 ulation involving uniform random sampling of 10,000 soil textures across the entire soil texture
159 ternary diagram and simulating SMC and VPR for each soil texture realization, for each of the four
160 recharge sites. Cumulative distribution functions for VPR are then obtained to determine values
161 of VPR at each simulation time, which correspond to probabilities of non-exceedance (PNE) of
162 10% and 90%, hereafter referred to as the P10 and P90, respectively.

163 *2.4.1. Conditioning using the observed soil moisture content (SMC) data*

164 The confidence limits for each VPR are constrained further by conditioning the SMAP to the
165 observed SMC data for each site. This is achieved as follows: The Nash and Sutcliffe (1970)
166 efficiency (NSE) criterion is determined for each realization whereby

$$\text{NSE} = 1 - \frac{\sum_{i=1}^N (o_i - m_i)^2}{\sum_{i=1}^N (o_i - \bar{o}_i)^2} \quad (1)$$

167 and N is the number of data points, o_i are the observed SMC data, m_i are the modeled SMC data,
 168 and \bar{o}_i is the mean of the observed SMC data.

169 All the Monte Carlo simulation realizations are ranked in terms of their NSE values. The
 170 highest NSE values correspond to those models that gave the most favorable comparison with
 171 the observed data. Conditioning is achieved by only retaining the top 10% realizations with the
 172 highest values of NSE. Cumulative distribution functions for VPR are then obtained to determine
 173 P10 and P90 values of VPR following conditioning.

174 *2.4.2. Conditioning using the UKSO soil texture data*

175 As discussed earlier, soil texture of the surface cover for each of the four sites has been deter-
 176 mined at a 1 km scale using the UKSO soil map. UKSO provide a soil texture classification for
 177 each location, which is defined in terms of a polygon on a soil texture ternary diagram (recall Fig.
 178 1). As a comparison to conditioning VPR using SMC data, simulated VPR is also conditioned
 179 using the UKSO soil texture data. This is achieved by redetermining the P10 and P90 VPR values
 180 from the aforementioned full Monte Carlo simulation, whilst only retaining those soil textures
 181 contained within the associated UKSO soil texture polygon.

182 3. Results

183 Fig. 2 shows the modeling results for Warren Farm. First consider the plots of SMC in Fig. 2a.
184 Note that the plotted lines represent the P10 and P90 results from the unconstrained Monte Carlo
185 simulation, the conditioning on the observed SMC data and the conditioning to the UKSO soil
186 texture classification for that site. For each of the three cases, the P10 and P90 are closely overlain
187 on top of each other suggesting that SMC is completely insensitive to soil texture. Furthermore,
188 the SMAP is able to estimate the observed SMC data to a considerably high-level, regardless of
189 the soil texture assumed.

190 In contrast, the unconstrained Monte Carlo simulation (the green envelope) presented in Fig.
191 2b suggests that soil texture has a much more significant effect on VPR, with the difference be-
192 tween the P10 and P90 results being as high as 50% during the peak event of 2004. The difference
193 between the P10 and P90 for VPR clearly narrow following conditioning to the observed SMC
194 data (consider the blue solid lines). However, even with this conditioning, the difference between
195 the P10 and P90 results are as high as 30% during the peak event of 2004. Conditioning the sim-
196 ulations using instead the UKSO soil texture classification leads to a similar level of refinement
197 on VPR. However, conditioning to the UKSO soil texture classification generally leads to a slight
198 overestimation of VPR in 2007 and 2008 as compared to the results obtained by conditioning to
199 SMC data with the exception of the peak VPR events of early 2007 and 2008.

200 Fig. 3 shows a very similar story for the Highfield Farm site. However, in this case, soil
201 texture conditioning leads to an underestimation of VPR as compared to results obtained by SMC
202 conditioning.

203 Figs. 4 and 5 show results from Beche Park Wood and Grimsbury Wood, respectively. SMC
204 sensitivity to soil texture is more apparent at these sites (consider the green envelopes in Figs. 4a
205 and 5a). However, SMC data estimates following SMC conditioning and soil texture conditioning
206 at both sites are virtually interchangeable. In contrast, as with Warren Farm and Highfield Farm,
207 there is a much wider variation in VPR estimate.

208 To gain further insight, Fig. 6 shows the location of all the simulations selected by the SMC
209 conditioning on a soil texture ternary diagram (the blue dots) for each of the four sites considered.
210 The polygons for the associated UKSO soil texture classifications for each of the sites are also
211 shown for comparison (the red solid lines).

212 From Figs. 6a and b, it is clear that for Warren Farm and Highfield Farm, SMC conditioning
213 identifies soil textures that are completely different to those suggested by UKSO. According to
214 Fig. 1, the SMC conditioning suggests that Warren Farm is more of a “clay to chalky loam” as
215 opposed to a “chalky, silty loam”. In the same way, the SMC conditioning suggests that Highfield
216 Farm is more of a “chalky silty loam” as opposed to a “loam to sand”.

217 In contrast, Figs. 6c and d show that some of the soil textures identified by SMC conditioning
218 exist within the allocated UKSO soil texture classification polygons for Beche Park Wood and
219 Grimsbury Wood. It is also notable that the soil log descriptions reported by Sorensen et al. (2014)
220 for these sites are closer to the UKSO descriptions as compared to the soil log descriptions for
221 Warren Farm and Highfield Farm. Recall Sorensen et al. (2014) describes Beche Park Wood as
222 gravely clay and Grimsbury Wood as silty clay. UKSO describe Beche Park Wood as “clay to
223 clayey loam” and Grimsbury Wood as “clay to silt”.

224 Fig. 7 shows contour plots of NSE across the soil texture ternary diagrams for each of the four

225 sites. Note that NSE values closer to one imply better fits to the observed SMC data. Only values
226 of NSE from 0.7 to 0.9 are contoured because 0.9 represents the highest NSE values achieved and
227 less than 0.7 is arguably too poor to consider. The first thing to note is that NSE values greater than
228 0.7 are achieved at all four sites for all soil textures outside of the UKSO “sand” polygon. Values
229 of NSE within the UKSO “sand” polygon were mostly less than 0.7 for each of the four localities.
230 The next thing to note is that at Warren Farm, NSE was between 0.86 and 0.9 for all soil textures,
231 excluding the UKSO “sand” polygon. NSE values were considerably lower but still exhibit little
232 variability with soil texture at Highfield Farm, Beche Park Wood and Grimsbury Wood.

233 **4. Discussion**

234 The most important observation that can be made from Figs. 2 to 5 is that SMC is virtually
235 insensitive to soil texture. On the other hand, vertical percolation rate exhibits a stronger depen-
236 dence on soil texture. The above results include a range of different soil type scenarios; consider
237 the UKSO texture classification polygons in Fig. 6. However, all the sites studied are situated
238 in Southern England, and therefore all experience a UK maritime climate. The extent to which
239 climate may be important on the above finding is discussed below.

240 From an earlier sensitivity analysis of the aforementioned SMAP, Mathias et al. (2015) found
241 that the ratio of AE to PE, averaged over 34 years, ranged from 40% to 94% over the entire soil
242 textural triangle (see their Fig. 5a). However, for sand fraction less than 90% this variation reduced
243 to between just 80% and 94%. The main reason for this is that, in a UK maritime climate, there
244 is generally sufficient rainfall to satisfy evaporative demands. Re-inspection of the governing
245 equations presented by Mathias et al. (2015) reveals that the impact of soil texture on SMC is

246 largely through its control on AE. Because AE is virtually the same regardless of soil texture in
247 this context, very little variation of SMC is observed with changing soil texture.

248 It is interesting to note that there is marginally more sensitivity of SMC to soil texture at Beche
249 Park Wood and Grimsbury Wood as compared to Warren Farm and Highfield Farm. The main
250 difference between the wooded sites and the farm sites, as far as the SMAP is concerned, is that
251 the wooded sites experience reduced net rainfall due to forest canopy interception losses. Figs.
252 2c, 3c, 4c and 5c show monthly mean AE (excluding canopy interception loss) and VPR. It is
253 clear that VPR is considerably lower at the wooded sites. Furthermore, whilst AE shows marginal
254 summer variability with soil texture at all four sites, winter variability in AE is only apparent at
255 the wooded sites.

256 The reduction in available rainfall due to canopy interception makes it harder for plant roots
257 to satisfy evaporative demands. Consequently, the system becomes more dependent on the soil
258 moisture relationship with matric potential and plant stress function (consider Eqs. (22) and (23)
259 in Mathias et al. (2015)). Hence SMC can be seen to be more variable with soil texture at the
260 wooded sites.

261 The wooded sites can be thought of as a proxy for a slightly more arid climate. It follows that
262 SMC is expected to exhibit a much greater sensitivity to soil texture in semi-arid and arid climates,
263 as compared to UK maritime climates.

264 With regards to the stronger sensitivity of VPR to soil texture as compared to SMC, VPR is
265 calculated by the SMAP using a non-linear function of SMC (Mathias et al., 2015, Eq. (20)).
266 It follows that any minor variability in SMC will naturally lead to a greater variability in VPR.
267 Conditioning the SMAP to the observed SMC data or the UKSO soil texture classifications leads

268 to a refining of the confidence limits for VPR. However, given the insensitivity of SMC to soil
269 texture, it does not follow that this conditioning leads to increased reliability with regards to VPR.

270 Similar to the JULES simulations presented by Sorensen et al. (2014), close to zero runoff was
271 estimated by all the models regardless of the soil texture adopted. At Warren Farm the models
272 estimated runoff to occur only on the 27th May 2007 and 20th July 2007 where recorded daily
273 rainfall was 59 and 105 mm, respectively. At the other three sites, runoff was estimated only to
274 occur on the 20th July 2007. Both of these dates have been previously recognized in terms of their
275 high rainfall intensity by Ireson et al. (2011). The reason that the May event is only found to be
276 significant at Warren Farm is due to its relative higher altitude and hence higher rainfall generally.
277 In fact surface runoff was likely to have occurred on many more occasions at Grimsbury Wood
278 and Beche Park Wood due to the nature of the overlying Paleogene deposits (Maurice et al., 2010).
279 However, the modelling approach applied here (and by Sorensen et al. (2014) when using JULES)
280 is not capable of estimating these events due to the use of daily rainfall, which leads to an averaging
281 on rainfall intensities over a 24 hour period (Mathias et al., 2015).

282 **5. Summary and conclusions**

283 In this study, four instrumented recharge monitoring sites previously presented by Sorensen et
284 al. (2014) are revisited to explore the value of observed SMC as a constraint for VPR (a proxy for
285 estimating groundwater recharge rate) estimation. The four sites represent a range of different soil
286 classifications. Although all four sites are from Southern England, two of the sites are located in
287 woodland areas, providing a proxy for a slightly more arid climate.

288 In their earlier study, Sorensen et al. (2014) concluded that SMC was not a good constraint in

289 this respect. The basis for their argument was that they used four different models to estimate the
290 SMC data and found that, although each model was “generally good” at estimating the SMC data,
291 the different models led to large variations of VPR.

292 In this article, the observed SMC data has been revisited using a single model structure, the
293 aforementioned SMAP, developed previously by Mathias et al. (2015). Furthermore, rather than
294 just using the SMAP to estimate both SMC and VPR, the model is also calibrated directly to
295 the SMC data to look at how such data can be used to reduce uncertainty associated with VPR
296 estimate.

297 Monte Carlo simulation using the SMAP suggests that aggregated SMC is virtually insensitive
298 to soil texture. In contrast, uncertainty in soil texture can lead to significant variations in VPR
299 prediction, as high as 50% of P10 values in some cases. Conditioning the SMAP to the observed
300 SMC data or the UKSO soil texture classifications leads to a refining of the confidence limits for
301 VPR. However, given the insensitivity of aggregated SMC to soil texture, it does not follow that
302 this conditioning leads to increased reliability with regards to VPR.

303 Using a goodness of fit measure, the NSE criterion, it was possible to delineate regions on a
304 soil texture ternary diagram that provide better correspondence between the SMAP and observed
305 SMC at each of the four sites (recall Fig. 6). Interestingly, the delineated regions did not all
306 coincide with the polygons associated with the UK soil observatory (UKSO, 2016) soil texture
307 classifications for the different sites. However, the regions defined by the NSE values represent
308 well defined shapes in all four cases, potentially pointing to an alternative method for defining a
309 “hydrological” soil texture for these sites.

310 Overall, it is found that the calibrated soil texture values from such an exercise do not always

311 coincide with data from existing field-scale soil texture maps. But more importantly, whilst un-
312 certainty in soil texture can lead to significant uncertainty in groundwater recharge estimation, it
313 is found that aggregated SMC is virtually insensitive to soil texture.

314 The insensitivity of aggregated SMC to soil texture is largely attributed to the fact that AE is
315 generally not much less than PE in UK maritime climates. However, it is hypothesized that much
316 greater sensitivity of aggregated SMC with soil texture would be observed in arid climates where
317 AE is likely to be much less than PE and more controlled by soil hydraulic properties.

318 **6. Acknowledgements**

319 We are very grateful for the useful comments provided by two anonymous reviewers.

320 **7. References**

- 321 Allen, R. G., Pereira, L. S., Raes D., Smith M. (1998), Crop evapotranspiration-guidelines for computing crop water
322 requirements. In FAO Irrigation and drainage, Paper 56, Rome.
- 323 Best, M. J., Pryor, M., Clark, D. B., Rooney, G. G., Essery, R., Mnard, C. B. et al. (2011), The Joint UK Land Environ-
324 ment Simulator (JULES), model description–Part 1: Energy and water fluxes, *Geoscientific Model Development*,
325 4, 677–699.
- 326 Cuthbert, M. O., Acworth, R. I., Andersen, M. S., Larsen, J. R., McCallum, A. M., Rau, G. C., Tellam, J. H. (2016),
327 Understanding and quantifying focused, indirect groundwater recharge from ephemeral streams using water table
328 fluctuations, *Water Resour. Res.*, 52, 827–840.
- 329 Feddes, R. A., Kowalik, P., Kolinska–Malinka, K., Zaradny, H. (1976). Simulation of field water uptake by plants
330 using a soil water dependent root extraction function. *J. Hydrol.*, 31, 13–26.
- 331 Gash, J. H. C., Lloyd, C. R., Lachaud, G. (1995), Estimating sparse forest rainfall interception with an analytical
332 model, *J. Hydrol.*, 170, 79–86.

333 Healy, R. W., Cook, P. G. (2002), Using groundwater levels to estimate recharge, *Hydrogeol. J.*, 10, 91–109.

334 Herbst, M., Rosier P. T. W., McNeil D. D., Harding R. J., Gowing D. J. (2008), Seasonal variability of interception
335 evaporation from the canopy of a mixed deciduous forest, *Agric. Forest Meteorol.*, 148, 1655–1667.

336 Ireson, A. M., Wheater, H. S., Butler, A. P., Mathias, S. A., Finch, J., Cooper, J. D. (2006), Hydrological processes in
337 the Chalk unsaturated zone—insights from an intensive field monitoring programme, *J. Hydrol.*, 330, 29–43.

338 Ireson, A. M., Butler, A. P. (2011), Controls on preferential recharge to Chalk aquifers, *J. Hydrol.*, 398, 109–123.

339 Kerry, R., Rawlins, B. G., Oliver, M. A., Lacinska, A. M. (2009), Problems with determining the particle size distri-
340 bution of chalk soil and some of their implications, *Geoderma*, 152, 324–337.

341 Lott, D. A., Stewart, M. T. (2016), Base flow separation: A comparison of analytical and mass balance methods, *J.*
342 *Hydrol.*, 535, 525–533.

343 Mathias, S. A., Butler, A. P. (2006), Linearized Richards’ equation approach to pumping test analysis in compressible
344 aquifers, *Water Resour. Res.*, 42, W06408.

345 Mathias, S. A., Skaggs, T. H., Quinn, S. A., Egan, S. N., Finch, L. E., Oldham, C. D. (2015), A soil moisture
346 accounting-procedure with a Richards’ equation-based soil texture-dependent parameterization, *Water Resour.*
347 *Res.*, 51, 506–523.

348 Mathias, S. A., McIntyre, N., Oughton, R. H. (2016), A study of non-linearity in rainfall-runoff response using 120
349 UK catchments, *J. Hydrol.*, 540, 423–436.

350 Maurice, L., Atkinson, T. C., Williams, A. T., Barker, J. A., Farrant, A. R. (2010), Catchment scale tracer testing from
351 karstic features in a porous limestone, *J. Hydrol.*, 389, 31–41.

352 Nash, J., & Sutcliffe, J. V. (1970), River flow forecasting through conceptual models part IA discussion of principles,
353 *J. Hydrol.*, 10, 282–290.

354 Quinn, S. A., Liss, D., Johnson, D., van Wonderen, J. J., and Power T. (2012), Recharge estimation methodologies
355 employed by the Environment Agency of England and Wales for the purposes of regional groundwater resource
356 modelling, *Geol. Soc. Spec. Publ.*, 364, 65–83.

357 Ragab, R., Finch, J., Harding, R. (1997), Estimation of groundwater recharge to chalk and sandstone aquifers using
358 simple soil models, *J. Hydrol.*, 190, 19–41.

359 Rutledge, A. T. (2007), Update on the use of the RORA program for recharge estimation, *Ground Water*, 45, 374–382.

360 Schaap, M. G., Leij, F. J., van Genuchten, M. T. (2001). Rosetta: A computer program for estimating soil hydraulic
361 parameters with hierarchical pedotransfer functions. *J. Hydrol.*, 251, 163–176.

362 Sorensen, J. P. R., Finch, J. W., Ireson, A. M., Jackson, C. R. (2014), Comparison of varied complexity models
363 simulating recharge at the field scale, *Hydrol. Process.*, 28, 2091–2102.

364 UK Soil Observatory (UKSO) (2016), Soil Texture, [ONLINE] Available at:
365 http://www.ukso.org/pmm/soil_texture.html [Accessed 17 October 2016].

366 van Genuchten, M. T. (1980), A closed-form equation for predicting the hydraulic conductivity of unsaturated soils.
367 *Soil Sci. Soc. Am. J.*, 44, 892–898.

368 von Freyberg, J., Moeck, C., Schirmer, M. (2015), Estimation of groundwater recharge and drought severity with
369 varying model complexity, *J. Hydrol.*, 527, 844–857.

370 **Appendix A. Ensuring stability for the Euler explicit time-stepping scheme**

371 This note provides additional information, not previously reported in Mathias et al. (2015),
372 concerning an Euler explicit time-stepping scheme for the simplified soil moisture accounting
373 procedure (SMAP).

374 The SMAP of concern involves solving the conservation problem (Mathias et al., 2015)

$$\frac{d\Theta}{dt} = q_r - q_{in} - q_{ro} - q_d - E_a \quad (\text{A.1})$$

375 where Θ [L] is the aggregated soil moisture content, t [T] is time, q_r [LT^{-1}] is the rainfall rate, q_{in}
376 [LT^{-1}] is the canopy interception rate, q_{ro} [LT^{-1}] is the surface runoff rate, q_d [LT^{-1}] is a drainage
377 rate (which forms an input into a linear reservoir store which outputs the vertical percolation) and
378 E_a [LT^{-1}] is the actual evapotranspiration rate.

379 Application of an Euler explicit time-stepping scheme leads to

$$\Theta_{n+1} = \Theta_n + \Delta t(q_{r,n} - q_{in,n} - q_{ro,n} - q_{d,n} - E_{a,n}) \quad (\text{A.2})$$

380 where Δt [T] is the chosen time-step

381 Following Appendix C of Mathias et al., (2016), it can be shown that stability of the above

382 scheme is ensured providing

$$\frac{\partial}{\partial \Theta}(-q_r + q_{in} + q_{ro} + q_d + E_a) < \frac{1}{\Delta t} \quad (\text{A.3})$$

383 Note that, according to the equations presented in Mathias et al., (2016), q_r , q_{in} and q_{ro} are

384 independent of Θ . The E_a term is jointly controlled by Θ and the potential evapotranspiration, E_p

385 [LT⁻¹]. It is found that the stability of the above scheme is largely insensitive to E_a , providing

386 E_a is constrained to ensure that $\Theta > \Theta_w$ where Θ_w [L] represents the minimum possible value of

387 Θ associated with plant wilting. In this way, the stability criterion in Eq. (A.3) can be simplified

388 further to

$$\frac{\partial q_d}{\partial \Theta} < \frac{1}{\Delta t} \quad (\text{A.4})$$

389 Mathias et al. (2015) prescribe that

$$q_d(S_e) = K_s S_e^\eta \left[1 - \left(1 - S_e^{1/m} \right)^m \right]^2 \quad (\text{A.5})$$

390 which is the hydraulic conductivity function for unsaturated soils originally proposed by van

391 Genuchten (1980). K_s [LT^{-1}] is the saturated hydraulic conductivity of the soil, η [-] and m [-]
 392 are empirical exponents, and S_e [-] is the effective saturation, estimated by the SMAP using

$$S_e = \frac{\Theta - \Theta_w}{\Theta_{pu}} \quad (\text{A.6})$$

393 where Θ_{pu} [L] is the soil moisture content capacity available for plant uptake.

394 Differentiating Eq. (A.5) with respect to Θ leads to

$$\frac{\partial q_d}{\partial \Theta} = \frac{K_s S_e^{\eta-1}}{\Theta_{pu}} \left[1 - \left(1 - S_e^{1/m} \right)^m \right]^2 \left[\eta + \frac{2S_e^{1/m} (1 - S_e^{1/m})^{m-1}}{1 - (1 - S_e^{1/m})^m} \right] \quad (\text{A.7})$$

395 Considering again Eq. (A.4), stability of the scheme is therefore ensured providing $\Theta < \Theta_0$

396 where

$$\Theta_0 = \Theta_{pu} S_0 + \Theta_w \quad (\text{A.8})$$

397 and S_0 is found iteratively from the expression

$$\frac{K_s S_0^{\eta-1}}{\Theta_{pu}} \left[1 - \left(1 - S_0^{1/m} \right)^m \right]^2 \left[\eta + \frac{2S_0^{1/m} (1 - S_0^{1/m})^{m-1}}{1 - (1 - S_0^{1/m})^m} \right] = \frac{1}{\Delta t} \quad (\text{A.9})$$

398 Note that Θ_0 only needs to be found once for each simulation because Θ_0 does not vary with time.

399 Following Mathias et al., (2016), the above constraint can be imposed by determining the

400 discrete values of q_d from

$$q_{d,n} = \begin{cases} 0, & \Theta_{trial} < 0 \\ q_{d,trial}, & 0 < \Theta_{trial} < \Theta_0 \\ \frac{\Theta_n - \Theta_0}{\Delta t} + q_{r,n} - q_{in,n} - q_{ro,n} - E_{a,n}, & \Theta_{trial} > \Theta_0 \end{cases} \quad (\text{A.10})$$

401 where

$$\Theta_{trial} = \Theta_n + \Delta t(q_{r,n} - q_{in,n} - q_{ro,n} - q_{d,trial} - E_{a,n}) \quad (\text{A.11})$$

402 with $q_{d,trial}$ being calculated directly from Eq. (A.5) with $S_e = S_{e,n}$.

403 The reader is referred to Mathias et al. (2015) for all other details concerning the SMAP.

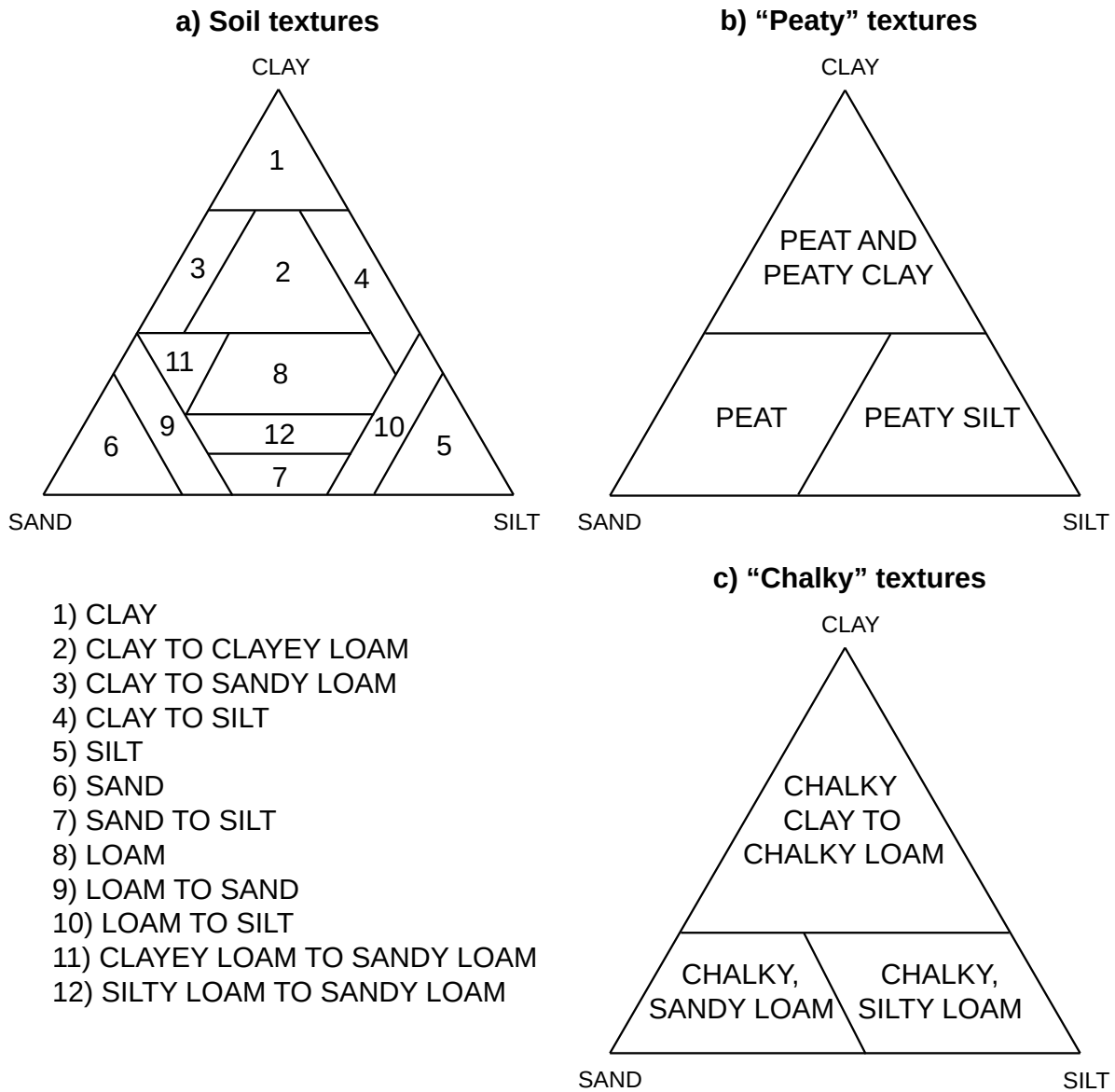


Figure 1: Soil texture ternary diagrams illustrating the various available UKSO soil texture classifications (adapted from UKSO, 2016).

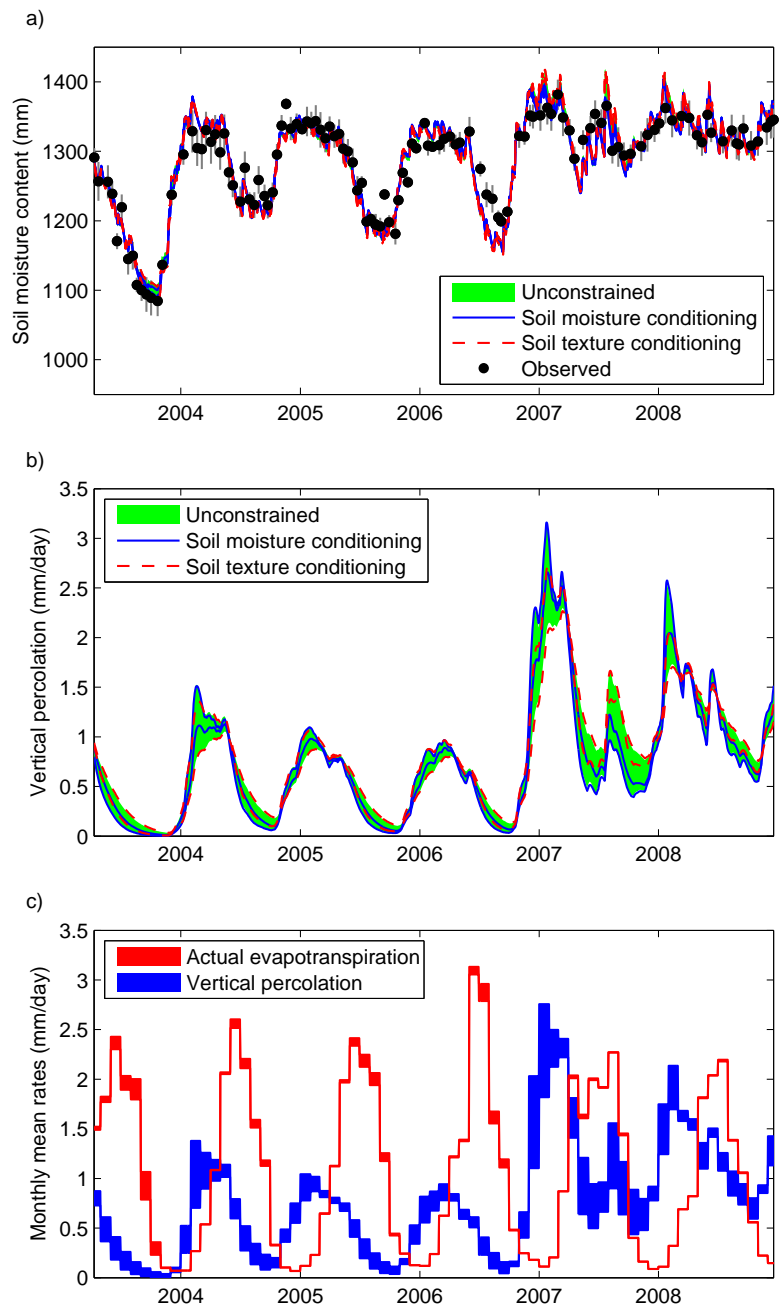


Figure 2: a) and b) Time-series plots of daily soil moisture content and daily vertical percolation rate for Warren Farm. The black dots are the observed soil moisture content data previously presented by Sorensen et al. (2014). The grey bars represent the range in observed soil moisture content, as reported by Sorensen et al. (2014). The green envelope represent the area bounded by the P10 and P90 from the Monte Carlo simulation obtained by uniform sampling across the entire soil texture ternary diagram. The blue lines represent the P10 and P90 of the top 10% of all the simulations in terms of their ability to simulate the observed soil moisture content data. The dashed red lines represent the P10 and P90 of all those simulations that contained soil textures within the UKSO polygon for this site. c) Time-series plots of monthly mean actual evapotranspiration (excluding canopy interception loss) and vertical percolation. The envelopes represent the area bounded by the P10 and P90 from the Monte Carlo simulation obtained by uniform sampling across the entire soil texture ternary diagram.

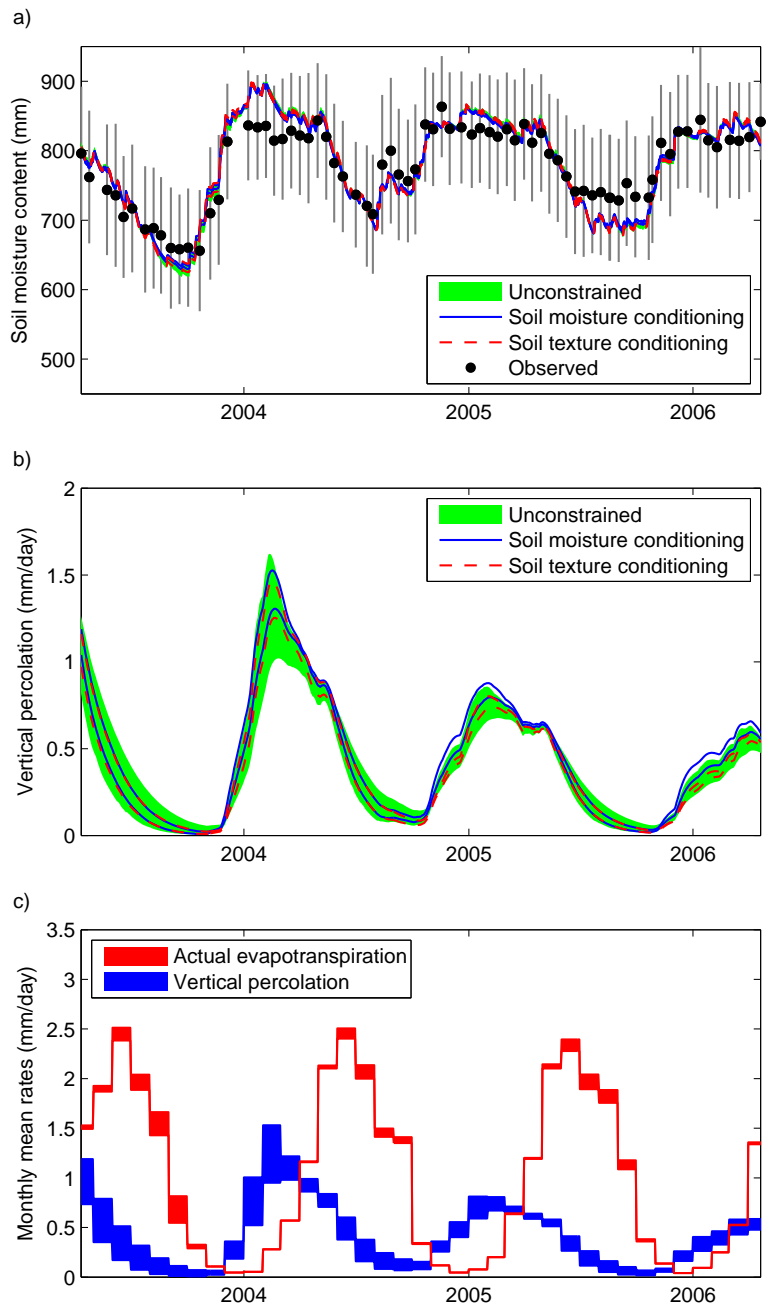


Figure 3: The same as Fig. 2 but for Highfield Farm.

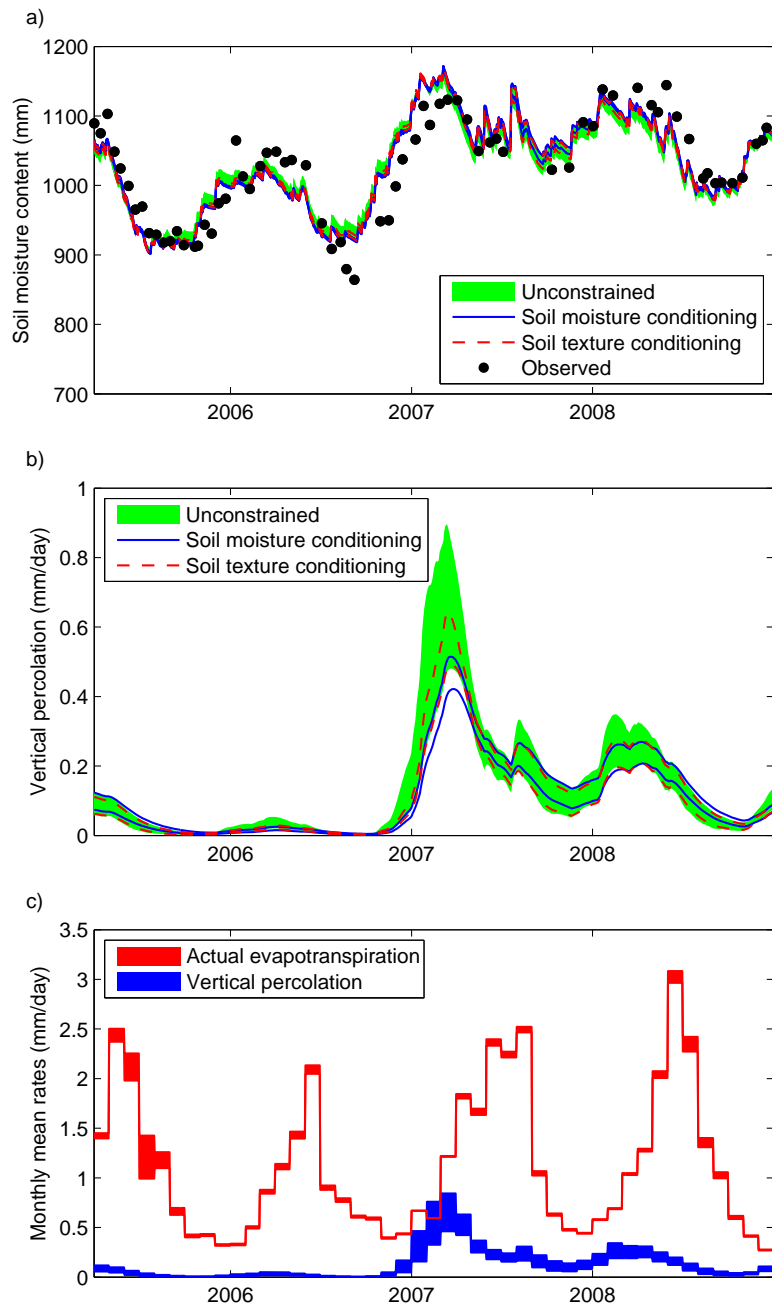


Figure 4: The same as Fig. 2 but for Beche Park Wood.

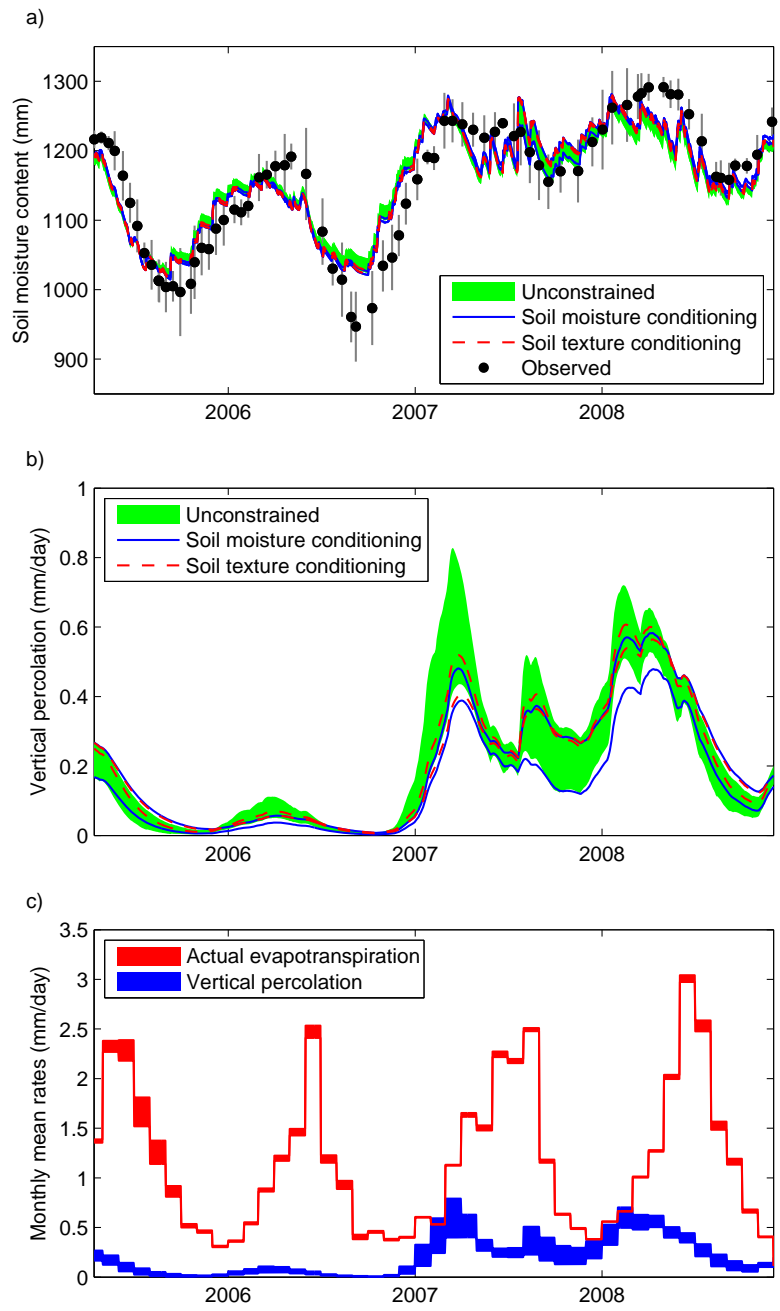


Figure 5: The same as Fig. 2 but for Grimsbury Wood.

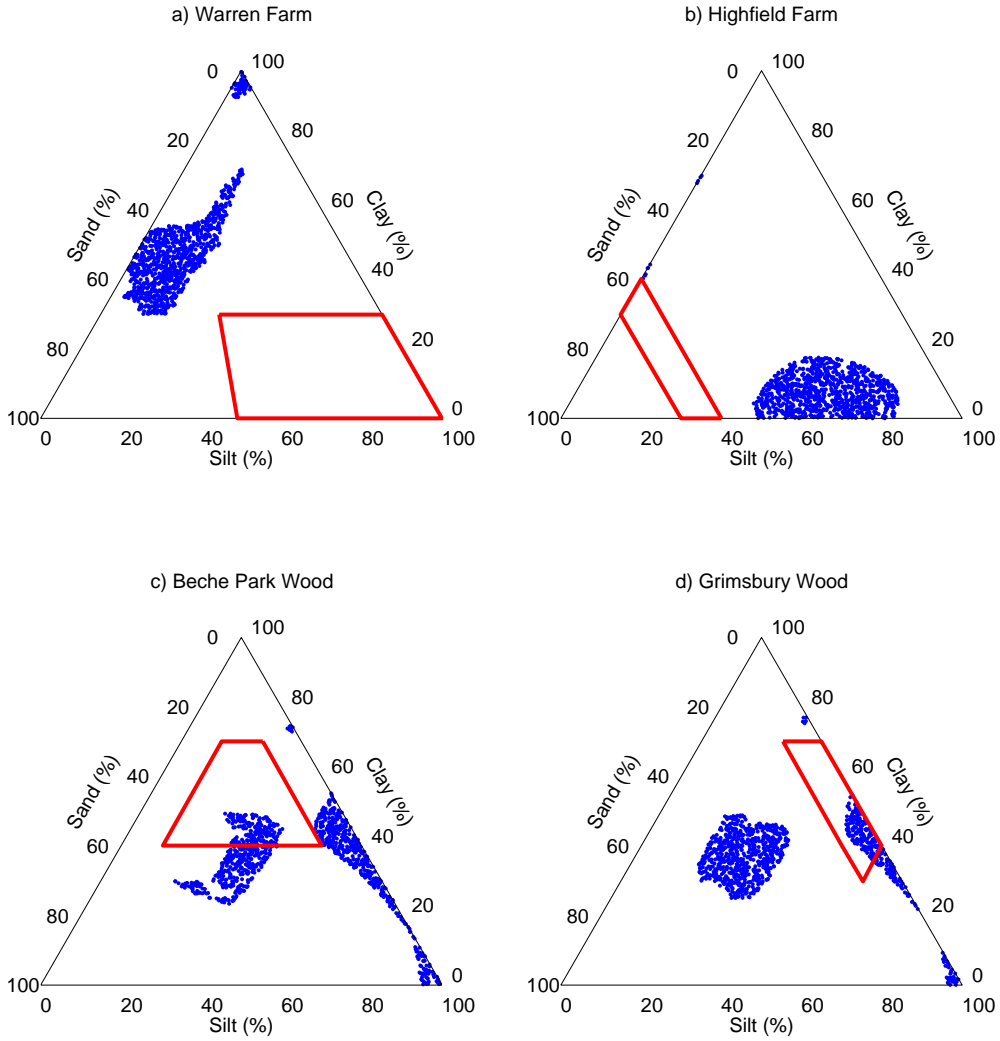


Figure 6: Soil texture ternary diagrams showing blue dots as the locations of the top 10% simulations (in terms of their ability to simulate the observed soil moisture data) for a) Warren Farm, b) Highfield Farm, c) Beche Park Wood and d) Grimsbury Wood. The red polygons denote the region defined by the UKSO soil texture classification associated with each of these sites.

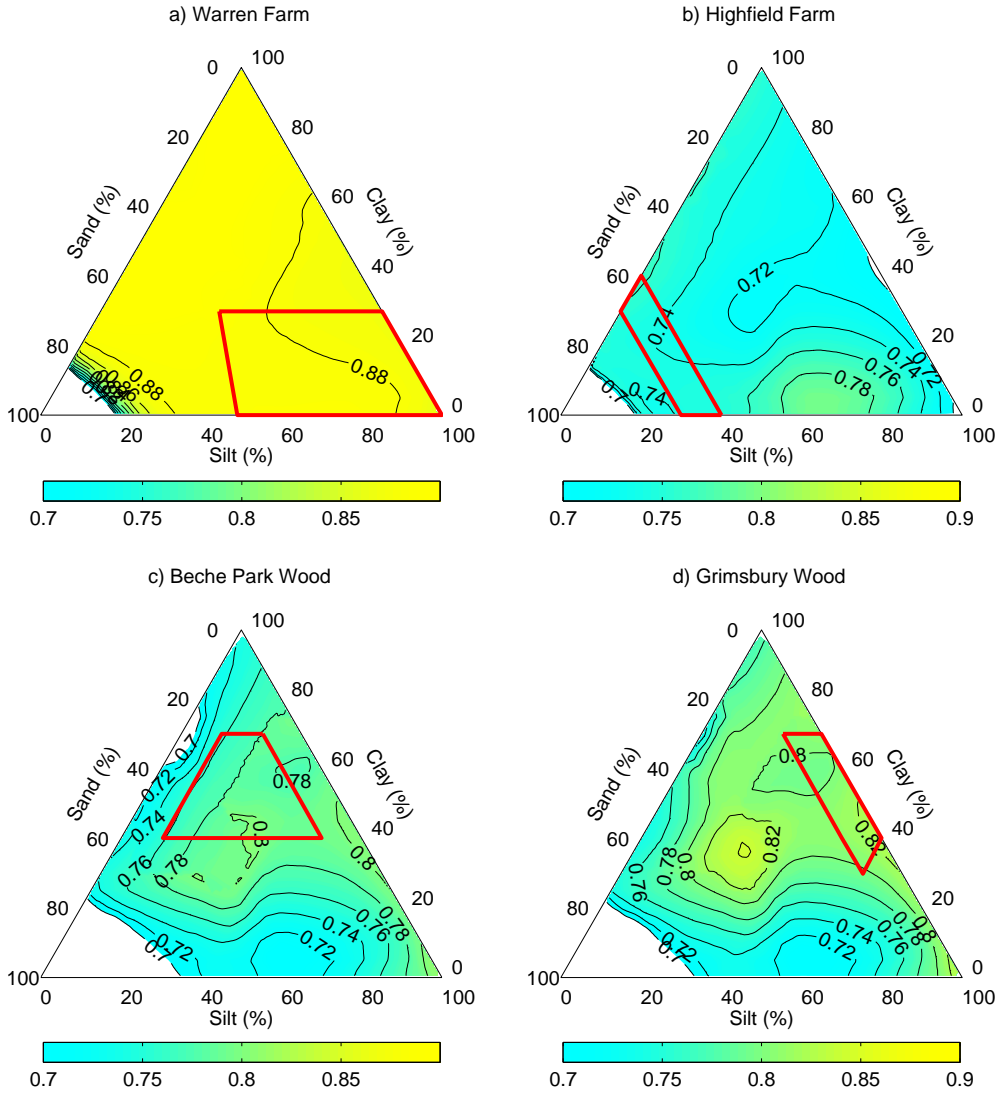


Figure 7: Soil texture ternary diagrams showing Nash and Sutcliffe (1970) efficiency (NSE) contours for a) Warren Farm, b) Highfield Farm, c) Beche Park Wood and d) Grimsbury Wood. The red polygons denote the region defined by the UKSO soil texture classification associated with each of these sites. The color bar values relate to NSE value as given in Eq. (1). Recall that NSE is used here to assess the ability of the models to simulate the observed soil moisture content data.